

Cite this: *Chem. Commun.*, 2012, **48**, 11692–11694

www.rsc.org/chemcomm

COMMUNICATION

Tailoring an alien ferredoxin to support native-like P450 monooxygenase activity†

Stephen G. Bell,^{*ab} James H. C. McMillan,^b Jake A. Yorke,^b Emma Kavanagh,^b Eachan O. D. Johnson^b and Luet-Lok Wong^{*b}

Received 17th August 2012, Accepted 11th October 2012

DOI: 10.1039/c2cc35968e

A ferredoxin associated with biological Fe–S cluster assembly has been remodelled to transfer electrons to a P450 enzyme and support substrate oxidation at 80% of the physiological ferredoxin activity, opening up the possibility of tailoring ferredoxins to reconstitute the activity of P450 enzymes for which the electron transfer partner proteins are not known.

Selective oxidation of carbon–hydrogen bonds in a complex organic molecule is a challenging reaction that has numerous applications in synthesis: complex routes can be simplified and one-step synthesis from readily available feedstocks becomes possible. Enzymatic oxidation is attractive because of the energy efficiency, mild conditions and the absence of heavy metal and toxic wastes. The cytochrome P450 (CYP) monooxygenases catalyse the oxidation of C–H bonds by dioxygen.¹



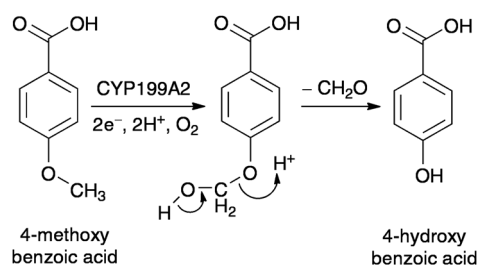
P450 enzymes oxidise diverse substrates ranging from alkanes to alicyclic and aromatic compounds, terpenes, amino acids and macrolides. Their potential applications extend beyond C–H bond oxidation as the enzymes also catalyse epoxidation, C–C bond formation and cleavage, dealkylation and desaturation.^{1b} With rising energy costs and environmental concerns there is an urgent need to expand the repertoire of P450-catalysed oxidation reactions for potential applications in sustainable synthesis.

The two electrons required for P450 activity are commonly supplied by NAD(P)H.¹ In bacteria, a flavin (FAD or FMN) dependent reductase accepts the two electrons and releases these to a redoxin that transfers them to the P450; common redoxins are [Fe–S] ferredoxins and FMN flavodoxins.² However, numerous CYP genes are orphaned in the genome—the genes encoding the electron transfer proteins are not located nearby in the DNA sequence and therefore not known. In

some cases the electron transfer partners are difficult to produce heterologously or are unstable. Functional studies and applications thus require testing of surrogate electron transport chains, *e.g.* putidaredoxin reductase/putidaredoxin (PdR/Pdx) of the P450cam system,^{3a} the adrenodoxin reductase/adrenodoxin (AdR/Adx) pair^{3b} and the FMN-[2Fe–2S] domain of P450Rh_f.^{3c} to reconstitute the P450 activity. Such crossover activities are either absent or typically 10- to 1000- fold lower than with the physiological electron transfer chain because of specific interactions in protein binding and electron transfer. We report here a new approach to overcoming this recognition barrier whereby a ferredoxin with low P450 electron transfer activity is engineered to attain a turnover rate of 19.4 s⁻¹ compared to 24 s⁻¹ for the physiological ferredoxin. The results establish essential roles for residues 36, 42–44 (cluster-binding loop), 66 and 73 (α3 helix) of the canonical vertebrate-type ferredoxin structure in ferredoxin–P450 binding and electron transfer and provide a blueprint for similar engineering efforts to support the activity of other P450 enzymes.

CYP199A2 from *Rhodospseudomonas palustris* CGA009 catalyses the oxidation of substituted benzoic acids at the *para*-position.⁴ The *RPA1871* gene for CYP199A2 is immediately followed by the *RPA1872* gene that encodes a [2Fe–2S] ferredoxin Pux which, in concert with the ferredoxin reductase PuR (*RPA3872*),^{4,5} supports the oxidative demethylation of 4-methoxybenzoic acid (Scheme 1) by CYP199A2 with $k_{\text{cat}} = 37.9 \text{ s}^{-1}$ and $K_{\text{m}} = 0.45 \mu\text{M}$.

R. palustris CGA009 has another [2Fe–2S] ferredoxin PuxB which shares high sequence identity with iron–sulfur cluster (*isc*) biogenic ferredoxins (Fig. S1, ESI†) such as Fdx from *Escherichia coli*, Etp1^{fd} from *Schizosaccharomyces pombe* and FdVI from *Rhodobacter capsulatus*,⁶ but supports 4-methoxybenzoic



Scheme 1 Oxidative demethylation of 4-methoxybenzoic acid catalysed by CYP199A2 from *Rhodospseudomonas palustris* CGA009.

^a The School of Chemistry and Physics, The University of Adelaide, North Terrace, Adelaide, SA 5005, Australia.

E-mail: stephen.bell@adelaide.edu.au; Fax: +61 8 8303 4380; Tel: +61 8 8313 4822

^b Department of Chemistry, University of Oxford, Inorganic Chemistry Laboratory, South Parks Road, Oxford OX1 3QR, UK.

E-mail: luet.wong@chem.ox.ac.uk; Fax: +44 (0)1865 272690; Tel: +44 (0)1865 272619

† Electronic supplementary information (ESI) available: Experimental details and supplementary figures. See DOI: 10.1039/c2cc35968e

Table 1 Reduction potentials (E vs. SHE) and kinetic parameters for CYP199A2-catalysed oxidation of 4-methoxybenzoic acid. The apparent Michaelis–Menten parameters k_{cat} and K_m were obtained at 30 °C under conditions where the first electron transfer from the ferredoxin to CYP199A2 is rate limiting (0.1 μM CYP199A2, 0.5–20 μM ferredoxin, 0.2 μM PuR, 1 mM 4-methoxybenzoic acid). The rate constant, k_f , for the formation of the $\text{Fe}^{\text{II}}(\text{CO})$ form and K_s , the dissociation constant for the formation of the Fdx/CYP199A2 complex, were obtained from stopped-flow experiments at 25 °C. N : NADH consumption rate under normal activity assay conditions with 0.5 μM CYP199A2, 5 μM Fdx and 1 μM PuR. All data are given as mean \pm S.D. for at least three independent experiments

Ferredoxin	N/s^{-1}	$k_{\text{cat}}/\text{s}^{-1}$	$K_m/\mu\text{M}$	E/mV	k_f/s^{-1}	$K_s/\mu\text{M}$
Pux ^{4a}	24.0 \pm 0.8	37.9 \pm 0.8	0.45 \pm 0.1	-251 \pm 2	30.9 \pm 0.7	0.48 \pm 0.08
PuxB ^{5a}	1.65 \pm 0.03	19.1 \pm 0.6	34.3 \pm 2.2	-291 \pm 4	—	—
PuxB/F73G	1.70 \pm 0.1	18.4 \pm 2.3	35.2 \pm 3.6	—	—	—
PuxB/M66D/A105V ^{5a}	2.53 \pm 0.1	22.7 \pm 1.4	36.4 \pm 3.6	—	—	—
PuxB/A42N/C43A/A44V/M66D/A105V = PuxB-5 ^{5a}	4.70 \pm 0.04	37.2 \pm 1.8	28.3 \pm 2.5	-293 \pm 2	—	—
PuxB-5/E36V	5.46 \pm 0.8	28.6 \pm 2.1	19.5 \pm 2.3	—	—	—
PuxB-5/F73G	13.5 \pm 1.1	30.9 \pm 1.1	3.8 \pm 0.4	-257 \pm 14	44.4 \pm 2.2	2.1 \pm 0.4
PuxB-5/E36V/F73G	19.4 \pm 0.7	34.1 \pm 0.8	2.0 \pm 0.2	-225 \pm 9	36.0 \pm 1.8	1.7 \pm 0.2
PuxB-5/E36V/F73G/M70L	14.1 \pm 0.9	27.3 \pm 0.5	1.4 \pm 0.1	-202 \pm 13	31.7 \pm 1.7	1.0 \pm 0.2
PuxB-5/E36V/F73G/R29S	13.4 \pm 0.3	32.5 \pm 0.5	3.5 \pm 0.2	—	—	—

acid oxidation by CYP199A2 with $k_{\text{cat}} = 19.1 \text{ s}^{-1}$ and $K_m = 34.3 \mu\text{M}$.^{5a} The high K_m value indicates poor complementarity between the interacting surfaces and leads to a NADH turnover rate of 1.65 s^{-1} in activity assays at a PuxB : CYP199A2 concentration ratio of 10 : 1, compared to 24.0 s^{-1} for Pux (Table 1).^{5a} Nevertheless, the reasonably high k_{cat} is a good basis for exploring ferredoxin–P450 recognition using PuxB as a molecular scaffold, replacing residues on the recognition surface with their counterparts in Pux.

The structure of PuxB (Fig. 1) is very similar to those of Fdx, FdVI and Etp1^{fd}, and the P450-associated ferredoxins Adx and Pdx.^{5a,6} Previous studies on Adx/CYP11A1 and Pdx/P450_{cam} binding suggested that ferredoxin surface residues in the $\alpha 3$ helix, the C-terminus of the $\alpha 1$ helix, the [Fe–S] cluster binding loop (residues 42–44 in PuxB), the C-terminus residue (A105 in PuxB), as well as residues aligning with Glu36 and Glu38 in PuxB were important for P450 binding.⁷ At the end of the $\alpha 1$ helix Arg29 in PuxB aligns with Ser29 in Pux (Fig. S1, ESI[†]). Within the $\alpha 3$ helix, Met66 in PuxB is Asp66 in Pux, Asp69 and Asp72 are conserved, Met70 aligns with Leu, while Phe73 is a Gly in Pux. Glu38 is conserved but Glu36 in PuxB is a Val in Pux.

Residues Ala42, Cys43, Ala44, Met66 and Ala105 in PuxB had been exchanged previously for their counterparts in Pux.^{5a}

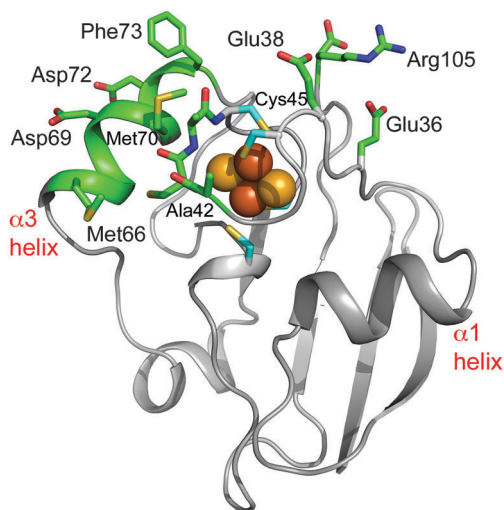


Fig. 1 The crystal structure of the A105R mutant of PuxB (pdb code: 3HUI) highlighting residues in the likely P450 recognition surface.

The M66D/A105V double mutant showed a similar K_m but slightly higher k_{cat} than wild type (WT) PuxB (Table 1). The A42N/C43A/A44V/M66D/A105V mutant (PuxB-5) has a k_{cat} of 37.2 s^{-1} , twice the value for the WT and identical to that for Pux but the K_m remained high (28.3 μM), leading to a NADH turnover rate of 4.70 s^{-1} that is *ca.* 20% of the activity of Pux (Table 1).^{5a} The k_{cat} value showed that the 42–44 triad of residues which shield the iron centre closest to the protein surface (Fig. 1 and S1, ESI[†]) is important in promoting electron transfer.^{2,7c} Residue mismatches elsewhere on the recognition surface leads to the high K_m value but once the complex is formed PuxB-5 is capable of transferring electrons to CYP199A2 at the same rate as the physiological ferredoxin. We therefore investigated whether mutations at other PuxB surface residues could lower the K_m .

Addition of the E36V mutation to the PuxB-5 variant tightened CYP199A2 binding, reducing K_m to 19.5 \pm 2.3 μM but k_{cat} was also lowered to 28.6 \pm 2.1 s^{-1} (Fig. 2, Table 1). On the other hand, the PuxB-5/F73G mutant had a dramatically lower K_m of 3.8 \pm 0.4 μM . Although k_{cat} was also reduced (30.9 \pm 1.1 s^{-1}), the lower K_m meant that the NADH turnover rate at a PuxB : CYP199A2 ratio of 10 : 1 was increased nearly 3-fold to 13.5 \pm 1.1 s^{-1} as a result of CYP199A2 being closer to saturation kinetics with this mutant. Adding both the E36V and F73G mutations to PuxB-5 lowered

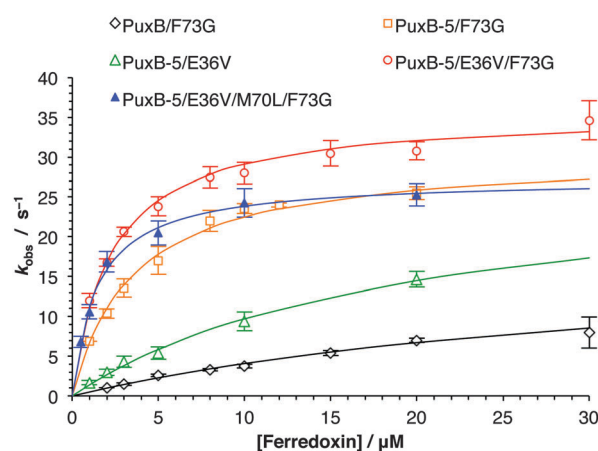


Fig. 2 Hyperbolic fits for kinetic titrations with PuxB mutants. See Table 1 for the fitted apparent k_{cat} and K_m values.

K_m to $2.0 \pm 0.2 \mu\text{M}$ and k_{cat} was $34.1 \pm 0.8 \text{ s}^{-1}$. The NADH turnover rate was $19.4 \pm 0.7 \text{ s}^{-1}$, 12 times that of WT PuxB and close to the 24.0 s^{-1} value for Pux. Interestingly, when the F73G mutation was introduced to WT PuxB, K_m was unchanged while k_{cat} was raised slightly. Adding the R29S mutation to the PuxB-5/E36V/F73G mutant lowered the activity while the M70L mutation lowered K_m ($1.4 \pm 0.1 \mu\text{M}$) but k_{cat} was also lowered ($27.3 \pm 0.5 \text{ s}^{-1}$), leading to a NADH turnover rate of 14.1 s^{-1} . All mutants showed the same product selectivity and similar efficiency of NADH utilisation for product formation as WT Pux and PuxB (data not shown).

These results are the first report of ferredoxin engineering to support native-like P450 activity and provide new insights into ferredoxin-P450 recognition. The E36V mutation lowered K_m slightly; P450-associated ferredoxins have a hydrophobic residue at this position close to the [2Fe–2S] cluster while *isc* ferredoxins have an acidic residue (Fig. S1, ESI†). The tipping point was the 7-fold lowering of K_m when the F73G mutation was introduced to the PuxB-5 mutant. The acidic residue at the 72 position in the $\alpha 3$ helix is important in P450 binding,^{2,7} and it is not surprising that the side chain volume at residue-73 has such an impact. An important observation is that the F73G mutation was only effective when combined with the mutations in the PuxB-5 mutant. Overall the data showed that ferredoxin–CYP199A2 binding requires collective residue matches at 36, 38, and 105 on one side of residues 42–44 in the cluster binding loop and residues 66, 69, 72 and 73 on the other side. Interestingly the effects of the R29S and M70L mutations indicate that perfect residue matches with the physiological ferredoxin is not required for activities that are useful in practice.

Intra-complex electron transfer from Pux and the most active PuxB mutants to CYP199A2 was studied by stopped-flow spectrophotometry. Pre-reduced ferredoxins were mixed with oxidised CYP199A2 in the presence of a saturating concentration of 4-methoxybenzoic acid under an atmosphere of carbon monoxide. Since CO binding to ferrous P450 is fast, the rate constant, k_f for the formation of the $\text{Fe}^{\text{II}}(\text{CO})$ species (Fig. S2, ESI†) is an accepted measure of the electron transfer rate constant, k_{et} . The similar k_f and k_{cat} values for Pux and the PuxB-5/F73G, PuxB-5/E36V/F73G and PuxB-5/E36V/F73G/M70L mutants (Table 1) showed that the first electron transfer was rate limiting for the CYP199A2 catalytic cycle, as observed for the archetypal P450cam system.¹ K_s showed similar magnitude and trend as K_m , confirming improved protein binding in the mutants.

The reduction potentials of CYP199A2, Pux, and WT and mutants of PuxB were determined by spectroelectrochemical titrations. CYP199A2 showed the classic shift from a potential of $-445 \pm 2 \text{ mV}$ for the substrate-free form to a more oxidising value of $-227 \pm 3 \text{ mV}$ on 4-methoxybenzoic acid binding (Fig. S3, ESI†), facilitating electron transfer from the ferredoxin.¹ The potential of Pux ($-251 \pm 2 \text{ mV}$) was similar to that of Pdx (-245 mV), while those of WT PuxB and the PuxB-5 mutant ($-291 \pm 4 \text{ mV}$ and $-293 \pm 2 \text{ mV}$, respectively) were *ca.* 40 mV more reducing (Fig. S4, ESI† Table 1). Adding the F73G mutation increased the PuxB-5 potential to $-257 \pm 14 \text{ mV}$ and this shifted further, to $-225 \pm 9 \text{ mV}$ for the PuxB-5/E36V/F73G and $-202 \pm 13 \text{ mV}$ for the PuxB-5/E36V/M70L/F73G mutant.

As the ferredoxin potential became less reducing there was a corresponding decrease in k_f , indicating that the thermodynamic driving force was an important factor in the observed trend in electron transfer rates and hence k_{cat} . We inferred that the higher thermodynamic driving force for CYP199A2 reduction by WT PuxB (*ca.* 40 mV more reducing than Pux) compensated for the likely lower donor–acceptor coupling and higher reorganisation energy for electron transfer arising from sub-optimal residue interactions. This led to a higher k_{et} and thus k_{cat} for supporting CYP199A2 turnover that partially overcame the high K_m , resulting in a readily detectable activity. Faster electron transfer from PuxB mutants to CYP199A2 should be possible if different amino acid substitutions can be found that lower K_m of PuxB-5 while maintaining the ferredoxin potential at more reducing values. Other *isc* ferredoxins with lower reduction potentials than PuxB, *e.g.* Fdx (-380 mV)^{6a} and Etp^{fd} (-353 mV),^{6c} may be even better starting points for P450 recognition engineering.

In summary, the results establish, for the first time, the principle of tailoring a non-physiological ferredoxin to support native-like P450 activity. The k_{cat} for PuxB reached a native-like value when residues 42–44 in the cluster binding loop matched those in Pux, and further increases in turnover activity came from improved protein binding to lower the K_m . Since the structures of *isc* and P450-associated ferredoxins are closely similar in the P450 recognition region, it should be possible to tailor other ferredoxins to reconstitute the activity of CYP199A2 and potentially other known and new P450 enzymes.

We thank the EPSRC, BBSRC, the Rhodes Trust and NSERC (Canada) for financial and studentship support of this work.

References

- (a) *Cytochrome P450: Structure, Mechanism, and Biochemistry*, ed. P. R. Ortiz de Montellano, Kluwer Academic/Plenum Press, New York, 3rd edn, 2005; (b) M. J. Cryle, J. E. Stok and J. J. De Voss, *Aust. J. Chem.*, 2003, **56**, 749; (c) I. G. Denisov, T. M. Makris, S. G. Sligar and I. Schlichting, *Chem. Rev.*, 2005, **105**, 2253.
- F. Hannemann, A. Bichet, K. M. Ewen and R. Bernhardt, *Biochim. Biophys. Acta*, 2007, **1770**, 330.
- (a) I. C. Gunsalus and G. C. Wagner, *Methods Enzymol.*, 1978, **52**, 166; (b) T. Kimura and K. Suzuki, *J. Biol. Chem.*, 1967, **242**, 485; (c) F. Sabbadin, R. Hyde, A. Robin, M. Delenne, S. Flitsch, N. Turner, G. Grogan and N. C. Bruce, *ChemBioChem*, 2010, **11**, 987.
- (a) S. G. Bell, N. Hoskins, F. Xu, D. Caprotti, Z. Rao and L. L. Wong, *Biochem. Biophys. Res. Commun.*, 2006, **342**, 191; (b) S. G. Bell, F. Xu, I. Forward, M. Bartlam, Z. Rao and L. L. Wong, *J. Mol. Biol.*, 2008, **383**, 561; (c) S. G. Bell, W. Yang, A. Tan, E. O. D. Johnson, W. Zhou, Z. Rao and L. L. Wong, *Dalton Trans.*, 2012, **41**, 8703.
- (a) S. G. Bell, F. Xu, E. O. D. Johnson, I. M. Forward, M. Bartlam, Z. Rao and L. L. Wong, *JBIC, J. Biol. Inorg. Chem.*, 2010, **15**, 315; (b) F. Xu, S. G. Bell, Y. Peng, E. O. D. Johnson, M. Bartlam, Z. Rao and L. L. Wong, *Proteins: Struct., Funct., Bioinform.*, 2009, **77**, 867.
- (a) Y. Kakuta, T. Horio, Y. Takahashi and K. Fukuyama, *Biochemistry*, 2001, **40**, 11007; (b) G. Sainz, J. Jakoncic, L. C. Sieker, V. Stojanoff, N. Sanishvili, M. Asso, P. Bertrand, J. Armengaud and Y. Jouanneau, *JBIC, J. Biol. Inorg. Chem.*, 2006, **11**, 235; (c) M. Bureik, B. Schiffler, Y. Hiraoka, F. Vogel and R. Bernhardt, *Biochemistry*, 2002, **41**, 2311; (d) B. Schiffler, M. Bureik, W. Reinle, E. C. Muller, F. Hannemann and R. Bernhardt, *J. Inorg. Biochem.*, 2004, **98**, 1229; (e) J. J. Muller, F. Hannemann, B. Schiffler, K. M. Ewen, R. Kappl, U. Heinemann and R. Bernhardt, *J. Inorg. Biochem.*, 2011, **105**, 957.
- (a) V. Y. Kuznetsov, T. L. Poulos and I. F. Sevrionkova, *Biochemistry*, 2006, **45**, 11934; (b) K. M. Ewen, M. Kleser and R. Bernhardt, *Biochim. Biophys. Acta*, 2011, **1814**, 111; (c) F. Hannemann, M. Rottmann, B. Schiffler, J. Zapp and R. Bernhardt, *J. Biol. Chem.*, 2001, **276**, 1369.